Isothermal Oxidation Kinetics of Unstabilized Polypropylene in the Molten State

S. Sarrabi, X. Colin, A. Tcharkhtchi

LIM (UMR-CNRS 8006), Arts et Métiers Paristech, 151 Boulevard de l'Hôpital, 75013 Paris, France

Received 30 November 2007; accepted 24 March 2008
DOI 10.1002/app.28534
Published online 7 August 2008 in Wiley InterScience (www.interscience.wiley.com).

ABSTRACT: This article is devoted to the elaboration of a nonempirical kinetic model for the thermal oxidation of molten unstabilized polypropylene (PP), which occurs typically at 170–250°C, a current temperature range for PP processing. The validity of the kinetic model has been successfully checked with the kinetic curves of mass changes and ketone group buildup of quasihomogeneously oxidized PP films (≈40 μm thick) at 190, 200, and 230°C in atmospheric air. The orders of magnitude of the model parameters, determined with the kinetic model as an inverse method, are physically reasonable. Large differences obtained between some rate constant values determined in this study for PP and published elsewhere for polyethylene are tentatively explained. © 2008 Wiley Periodicals, Inc. J Appl Polym Sci 110: 2030–2040, 2008

Key words: ageing; kinetics (polym.); modeling; poly (propylene); (PP)

Polypropylene (PP) thermal oxidation has been intensively studied in the past half-century, but essentially in the solid state (typically in the temperature range of 40–150°C).[1–4] In this domain, the oxidation mechanism is relatively well elucidated: it is a radical chain reaction initiated by its main oxidation product, the hydroperoxide species POOH.[5] Nonempirical kinetic models have been recently derived from this closed-loop mechanism and successfully validated in large domains of temperatures and oxygen partial pressures.[6,7]

The problem that still remains open in this field is the choice of a relevant set of rate constant values because it has been well demonstrated that several possible sets can be used to simulate relatively simple kinetic curves, such as the oxygen uptake, ketone and hydroxyl group buildup, or mass changes.[8] A solution consisting of multiplying the number of experimental validation criteria has been recently proposed in the case of rubber thermal oxidation.[9] However, its application requires the realization of heavy experimental campaigns.

Curiously, despite the relative simplicity of the material structure (no crystallinity) and the increasing craze, few publications have been devoted to PP thermal oxidation in the molten state[10,11] in the last 2 decades for studies on polymer degradation during processing or mechanical recycling. In the case of PP rotational molding, the study of thermal oxidation is indispensable because of the sensitivity of this polymer at high temperatures.

The aims of this research are twofold:

- To establish a realistic mechanistic scheme for the thermal oxidation of molten PP, which typically occurs at 170–250°C, a current temperature range for PP processing.
- To derive from this scheme a nonempirical kinetic model allowing us to simulate satisfyingly, with a realistic set of rate constant values, experimental kinetic curves obtained at 190, 200, and 230°C.

THEORY

Mechanistic scheme

Up to now, all the mechanistic schemes proposed to describe the global trends of the thermal oxidation kinetics of polymers have been based on the standard scheme established in the 1940s by the Rubber and Plastics Research Association.[12] There is a general consensus on the propagation, which should be composed of two elementary steps:

$$P^{\bullet} + O_2 \xrightarrow{k_2} PO_2^{\bullet}$$

$$PO_2^{\bullet} + PH \xrightarrow{k_3} POOH + P^{\bullet}$$

The first reaction is very fast ($k_2 = 10^8$–10^9 L mol^{-1} s^{-1}),[13] whereas the second one depends

Correspondence to: S. Sarrabi (salah.sarrabi-2@etudiants.ensam.fr).

mainly on the abstractability of the involved hydrogen atom.[14] In the case of PP, hydrogen abstraction occurs selectively on methynes (tertiary CH groups):

At a high temperature (typically ≥180°C), at least three initiation modes have to be considered. The first two are unimolecular and bimolecular hydroperoxide decompositions:[15]

$$\mathrm{POOH} \xrightarrow{k_{1u}} 2\mathrm{P}^{\bullet}$$

$$\mathrm{POOH} + \mathrm{POOH} \xrightarrow{k_{1b}} \mathrm{P}^{\bullet} + \mathrm{PO_2}^{\bullet}$$

The third is a possible direct reaction of oxygen (a biradical) with the polymer:[16,17]

$$\mathrm{PH} + \mathrm{O_2} \xrightarrow{k_i} \mathrm{P}^{\bullet} + \mathrm{HO_2}^{\bullet}$$

Both hydroperoxide decompositions lead to $\mathrm{PO}^{\bullet}$ radicals. An important peculiarity of these radicals is that they can abstract hydrogen to give alcohols

or rearrange by β scission to give ketones:

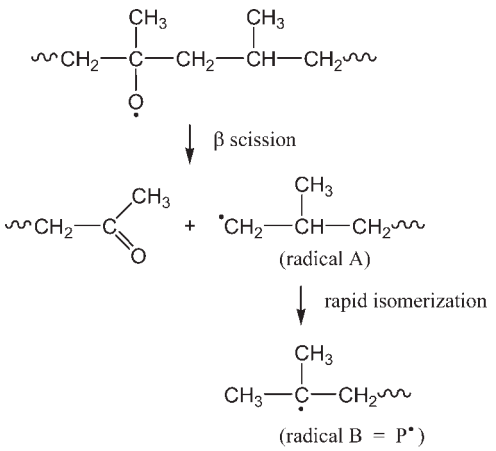

The unimolecular decomposition can be written as follows:

$$\begin{aligned}\mathrm{POOH} &\xrightarrow{k_{1u}} \mathrm{PO}^{\bullet} + {}^{\bullet}\mathrm{OH}\\ \mathrm{HO}^{\bullet} + \mathrm{PH} &\longrightarrow \mathrm{H_2O} + \mathrm{P}^{\bullet}\\ \mathrm{PO}^{\bullet} + \mathrm{PH} &\longrightarrow \mathrm{P{-}OH} + \mathrm{P}^{\bullet}\\ \mathrm{PO}^{\bullet} &\longrightarrow \mathrm{P{=}O} + \mathrm{P}^{\bullet} + w\mathrm{V}\ (-\mathrm{PH})\end{aligned}$$

where V is an average volatile compound, voluntarily distinguished from water, that is formed by β scission with yield w.

It is licit to write a balance reaction with k_{1u} as the corresponding rate constant because the homolytic rupture of the O—O bond is largely slower than the three following steps. Indeed, $\mathrm{PO}^{\bullet}$ and $\mathrm{HO}^{\bullet}$ radicals are very reactive and thus are almost instantaneously transformed into $\mathrm{P}^{\bullet}$ radicals. As a result, they are never seen by electron spin resonance spectrometry because their lifetime is too brief (on the contrary, $\mathrm{PO_2}^{\bullet}$ radicals can survive several days or even several weeks at the ambient temperature).

The balance reaction is thus

$$\mathrm{POOH} \xrightarrow{k_{1u}} \mathrm{H_2O} + 2\mathrm{P}^{\bullet} + (1-\gamma_1)\mathrm{P{-}OH} + \gamma_1\mathrm{P{=}O} + v\mathrm{V}\ (-(2-\gamma_1)\mathrm{PH})$$

where γ_1 and v are the respective yields of ketone P=O and volatile compound V.

In the same way, the bimolecular decomposition can be written:

$$\begin{aligned}2\mathrm{POOH} &\xrightarrow{k_{1b}} \mathrm{PO}^{\bullet} + \mathrm{PO_2}^{\bullet} + \mathrm{H_2O}\\ \mathrm{PO}^{\bullet} + \mathrm{PH} &\longrightarrow \mathrm{P{-}OH} + \mathrm{P}^{\bullet}\\ \mathrm{PO}^{\bullet} &\longrightarrow \mathrm{P{=}O} + \mathrm{P}^{\bullet} + w\mathrm{V}\ (-\mathrm{PH})\end{aligned}$$

Therefore, the balance reaction is

$$2\mathrm{POOH} \xrightarrow{k_{1b}} \mathrm{H_2O} + \mathrm{P}^{\bullet} + \mathrm{PO_2}^{\bullet} + (1-\gamma_1)\mathrm{P{-}OH} + \gamma_1\mathrm{P{=}O} + v\mathrm{V}((1-\gamma_1)\mathrm{PH})$$

There is no reason to assume that $\mathrm{PO}^{\bullet}$ radicals behave differently in the two initiation processes. Because they are formed with the same concentration, the yields γ_1 and v will take, in a first approach, values independent of the initiation process.

On the contrary, hydrogen abstraction by oxygen leads to alkyl radicals.[16,17] However, it is suspected that very reactive $\mathrm{HO_2}^{\bullet}$ radicals also abstract hydrogen to produce oxygenated water:

$$\begin{aligned}\mathrm{PH} + \mathrm{O_2} &\xrightarrow{k_i} \mathrm{P}^{\bullet} + \mathrm{HO_2}^{\bullet}\\ \mathrm{HO_2}^{\bullet} + \mathrm{PH} &\longrightarrow \mathrm{H_2O_2} + \mathrm{P}^{\bullet}\end{aligned}$$

Therefore, the balance reaction could be

$$\mathrm{PH} + \mathrm{O_2} \xrightarrow{k_i} 2\mathrm{P}^{\bullet} + \mathrm{H_2O_2}(-\mathrm{PH})$$

Because of the rapid isomerization of primary radicals (A) into tertiary ones (B),[18] it is assumed, in a

first approach, that termination will involve only tertiary radicals:

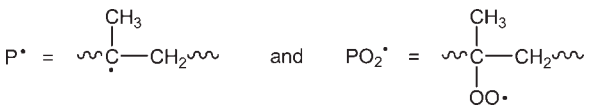

Tertiary alkyl radicals can undergo coupling or disproportionation according to

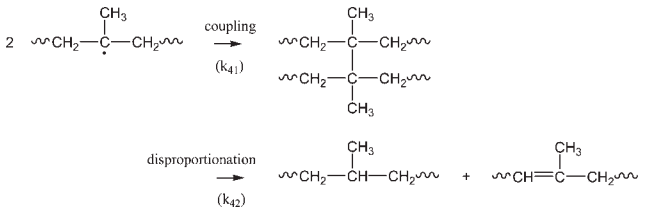

K is rate constant.

In this case, the termination can be described as follows:

$$P^{\bullet} + P^{\bullet} \xrightarrow{k_4} \gamma_4 P\text{—}P + (1-\gamma_4)PH + (1-\gamma_4)F$$

where F represents a double bond and γ_4 is the yield of alkyl–alkyl (P—P) bridges:

$$\gamma_4 = \frac{k_{41}}{k_4}$$

Here, $k_4 = k_{41} + k_{42}$.

In the same way, the termination between tertiary alkyl and tertiary peroxyl radicals can be described:

$$P^{\bullet} + PO_2^{\bullet} \xrightarrow{k_5} \gamma_5\,POOP + (1-\gamma_5)POOP + (1-\gamma_5)F$$

where γ_5 is the yield of peroxide (POOP) bridges.

In contrast, tertiary peroxyl radicals will undergo only coupling as a termination process:

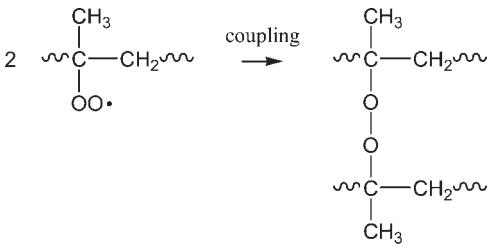

However, such termination cannot be very efficient, as recently shown in the case of polyethylene (PE) thermal oxidation.[19] It seems thus reasonable to consider, in a first approach, that a nonnegligible part of the radical pairs could escape from the cage to initiate new oxidation chains:

$$PO_2^{\bullet} + PO_2^{\bullet} \xrightarrow{k_{60}} [PO^{\bullet}\ {}^{\bullet}OP]_{cage} + O_2$$

$$[PO^{\bullet}\ {}^{\bullet}OP]_{cage} \xrightarrow{k_{61}} POOP$$

$$[PO^{\bullet}\ {}^{\bullet}OP]_{cage} \xrightarrow{k_{63}} 2P^{\bullet} + 2\gamma_1 P{=}O + 2(1-\gamma_1)P\text{—}OH + 2v\,V\ (-2PH)$$

Finally, a realistic mechanistic scheme for the thermal oxidation of molten unstabilized PP can be written:

$$PH + O_2 \xrightarrow{k_i} 2P^{\bullet} + H_2O_2\ (\text{—}PH)$$

$$POOH \xrightarrow{k_{1u}} H_2O + 2P^{\bullet} + (1-\gamma_1)P\text{—}OH + \gamma_1 P{=}O + v\,V\ (-(2-\gamma_1)PH)$$

$$2POOH \xrightarrow{k_{1b}} H_2O + P^{\bullet} + PO_2^{\bullet} + (1-\gamma_1)P\text{—}OH + \gamma_1 P{=}O + v\,V\ ((1-\gamma_1)PH)$$

$$P^{\bullet} + O_2 \xrightarrow{k_2} PO_2^{\bullet}$$

$$PO_2^{\bullet} + PH \xrightarrow{k_3} POOH + P^{\bullet}$$

$$P^{\bullet} + P^{\bullet} \xrightarrow{k_4} \gamma_4 P\text{—}P + (1-\gamma_4)PH + (1-\gamma_4)F$$

$$P^{\bullet} + PO_2^{\bullet} \xrightarrow{k_5} \gamma_5 POOP + (1-\gamma_5)POOP + (1-\gamma_5)F$$

$$PO_2^{\bullet} + PO_2^{\bullet} \xrightarrow{k_{60}} [PO^{\bullet}\ {}^{\bullet}OP]_{cage} + O_2$$

$$[PO^{\bullet}\ {}^{\bullet}OP]_{cage} \xrightarrow{k_{61}} POOP$$

$$[PO^{\bullet}\ {}^{\bullet}OP]_{cage} \xrightarrow{k_{63}} 2P^{\bullet} + 2\gamma_1 P{=}O + 2(1-\gamma_1)P\text{—}OH + 2v\,V\ (-2PH)$$

Volatile compounds

Up to now, polymer oxidation kinetics have been modeled with the polymer considered a quasiclosed system. Among the volatile products formed during oxidation, only water is removed from the polymer elemental composition.[6,7] However, if the polymer undergoes a strong mass loss, as evidenced in the case of PP thermal oxidation at relatively high temperatures (Fig. 1),[20] one should expect the other volatile products to also strongly affect the polymer elemental composition.

Careful analytical investigations have allowed the determination of the nature of the volatile products formed during PP thermal oxidation in the solid state (typically in the temperature range of 120–140°C).[21,22] Four volatile products have been clearly identified—acetone, acetaldehyde, methyl acrolein,

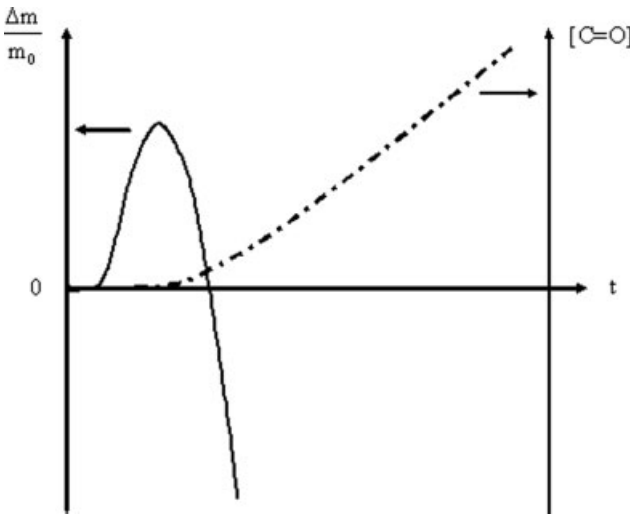

Figure 1 Schematic shape of the kinetic curves of mass changes and ketone group buildup for unstabilized PP films (100 μm thick) at 150°C in atmospheric air.[20]

and methyl ethyl ketone—but acetone is by far the main compound. Indeed, it represents more than 40 mol % of the total amount of generated gases.

Moreover, the rapid isomerization of primary radicals (A) into tertiary ones (B) is expected to induce a zip process (similar to depolymerization) in which each alkoxyl radical rearrangement (by β scission) leads to the formation of one acetone molecule. As a result, the acetone yields (w and v) in reactions involving k_{1u}, k_{1b}, and k_{63} are expected to depend on the kinetic chain length of the zip process and therefore to eventually take high values:

$w \lesssim 1$ per β scission event.
$v \lesssim \gamma_1$ per POOH decomposition event.

Kinetic model

A realistic kinetic model for the thermal oxidation of molten unstabilized PP must take into account the chemical changes due to the high amount of volatile product formation. In a first approach, the formation of secondary compounds (e.g., acetaldehyde, methyl acrolein, or methyl ethyl ketone) will be neglected. Thus, the new kinetic model [eqs. (1)–(9)] can be written as follows:

$$\frac{d[P^\bullet]}{dt} = 2k_i[PH][O_2] + 2k_{1u}f_{PH}[POOH] + k_{1b}f_{PH}[POOH]^2 - k_2[P^\bullet][O_2] + k_3[PO_2^\bullet][PH] - 2k_4[P^\bullet]^2 - k_5[P^\bullet][PO_2^\bullet] + 2k_{63}f_{PH}[PO^\bullet{}^\bullet OP] \quad (1)$$

$$\frac{d[PO_2^\bullet]}{dt} = k_{1b}f_{PH}[POOH]^2 + k_2[P^\bullet][O_2] - k_3[PO_2^\bullet][PH] - k_5[P^\bullet][PO_2^\bullet] - 2k_{60}[PO_2^\bullet]^2 \quad (2)$$

$$\frac{d[POOH]}{dt} = -k_{1u}f_{PH}[POOH] - 2k_{1b}f_{PH}[POOH]^2 + k_3[PO_2^\bullet][PH] + (1-\gamma_5)k_5[P^\bullet][PO_2^\bullet] \quad (3)$$

$$\frac{d[PO^\bullet{}^\bullet OP]}{dt} = k_{60}[PO_2^\bullet]^2 - (k_{61} + k_{63}f_{PH})[PO^\bullet{}^\bullet OP] \quad (4)$$

$$\frac{d[PH]}{dt} = -k_i[PH][O_2] - (2 - \gamma 1 + n_{PH}.v)k_{1u}f_{PH}[POOH] - (1-\gamma 1 + n_{PH}.v)k_{1b}f_{PH}[POOH]^2 - k_3[PO_2^\bullet][PH] + (1-\gamma_4)k_4[P^\bullet]^2 - 2(1+n_{PH}.v)k_{63}f_{PH}[PO^\bullet{}^\bullet OP] \quad (5)$$

$$\frac{\partial[O_2]}{\partial t} = D_{O2}\frac{\partial^2[O_2]}{\partial x^2} - k_2[P^\bullet][O_2] + k_{60}[PO_2^\bullet]^2 \quad (6)$$

$$\frac{d[P{=}O]}{dt} = (\gamma_1 - n_{CO}.v)k_{1u}f_{PH}[POOH] + (\gamma_1 - n_{CO}.v)k_{1b}f_{PH}[POOH]^2 + 2(\gamma_1 - n_{CO}.v)k_{63}f_{PH}[PO^\bullet{}^\bullet OP] \quad (7)$$

$$\frac{d[P{-}{-}OH]}{dt} = -(\gamma_1 + n_{OH}.v)k_{1u}f_{PH}[POOH] - (1+\gamma_1+n_{OH}.v)k_{1b}f_{PH}[POOH]^2 + k_3[PH][PO_2^\bullet] + (1-\gamma_5)k_5[P^\bullet][PO_2^\bullet] + 2(1-\gamma_1-n_{OH}.v) \times k_{63}f_{PH}[PO^\bullet{}^\bullet OP] \quad (8)$$

Weight changes are determined from a balance equation of the weight increase due to oxygen consumption and the weight loss due to volatile compound emissions:

$$\frac{1}{m_0}\frac{dm}{dt} = -\frac{32}{\rho_T}\frac{d[O_2]}{dt} - \frac{34}{\rho_T}\frac{d[H_2O_2]}{dt} - \frac{18}{\rho_T}\frac{d[H_2O]}{dt} - \frac{M_V}{\rho_T}\frac{d[V]}{dt}$$

Therefore

$$\frac{1}{m_0}\frac{dm}{dt} = +\frac{32}{\rho_T}(k_i[PH][O_2] + k_2[O_2][P^\bullet] - k_{60}[PO_2^\bullet]^2) - \frac{34}{\rho_T}(k_i[PH][O_2]) - \frac{18}{\rho_T}(k_{1u}f_{PH}[POOH] + k_{1b}f_{PH}[POOH]^2) - v\frac{M_V}{\rho_T}(k_{1u}f_{PH}[POOH] + k_{1b}f_{PH}[POOH]^2 + 2k_{63}f_{PH}[PO^\bullet{}^\bullet OP]) \quad (9)$$

In these equations

- γ_1 is the yield of ketones.
- γ_4 and γ_5 are the respective yields of alkyl–alkyl and peroxyl bridges.
- v is the yield of volatile product formation.
- M_V is the molar mass of the average volatile compound.

- D_{O2} is the oxygen diffusivity.
- n_{CO}, n_{OH}, and n_{PH} are the respective numbers of ketone, hydroxyl groups, and methynes in the volatile compound.
- f_{PH} is a mathematical function introduced into the system of differential equations to prevent, at high conversions, the substrate concentration from becoming negative.[23] In a first approach, a simple hyperbolic function was chosen to explain the variation of f_{PH} versus the PH concentration:

$$f_{PH} = \frac{[PH]}{[PH] + \varepsilon}$$

where typically $\varepsilon = 10^{-2} \ll 1$. This function does not introduce significant changes before a conversion value of about 99%.

- ρ_T is the density of molten PP. It corresponds to the density of the amorphous phase at temperature T. It was estimated from the density of the amorphous phase at the ambient temperature:

$$\rho_T = \frac{\rho_{298K}}{1 + \alpha_L(T - 298)}$$

where ρ_{298K} is 854 g/L[24] and α_L is the coefficient of cubic dilatation of the amorphous phase ($\alpha_L = 1.5 \times 10^{-4}$ K^{-1}). At 200°C, the numerical application gives $\rho_{473K} = 832$ g/L.

First of all, the system, composed of eqs. (1)–(6), was solved numerically with ODE23s Solver (Matlab), which is recommended for the resolution of stiff problems of chemical kinetics, with the following boundary conditions:

- In the sample thickness (at any x) when $t = 0$:

$$[P] = [PO_2^{\bullet}] = [PO^{\bullet}{}^{\bullet}OP] = 0\,\text{mol/L}$$

$$[POOH] = [POOH]_0 = 10^{-3} - 10^{-2}\,\text{mol/L}$$

$$[PH] = [PH]_0 \quad (\text{concentration of tertiary CH groups})$$

$$[O_2] = [O_2]_0 = P_{O2} \times S \quad (\text{Henry's law})$$

where P_{O2} is the oxygen pressure in the oxidizing atmosphere and S is the oxygen solubility coefficient for the polymer.

- At the sample surface in contact with atmospheric air (at $x = L$) when $t > 0$:

$$[O_2] = [O_2]_S = P_{O2} \times S \quad (\text{Henry law})$$

where $[O_2]_S$ is the equilibrium oxygen concentration.

TABLE I
Some Characteristics of the As-Received PP Powder

Characteristic	Technique (conditions)	Value	Unit
M_w	SEC	290	kg/mol
T_f	DSC (N_2, 10°C/min)	167	°C
T_C	DSC (N_2, 10°C/min)	110	°C
IsoT	IR (transmission)	66	%
L_C	DSC (N_2, 10°C/min)	7.3	Nm

isoT = isotacticity; L_C = crystalline lamella thickness; M_w = weight-average molar mass; T_C = crystallization temperature; T_f = melting point.

- At the sample surface in contact with one surface impermeable to oxygen (at $x = -L$) when $t > 0$:

$$\text{Oxygen flow through the polymer} - \text{Aluminum cup interface} = 0$$

The system of eqs. (1)–(6) gave access to the spatial distribution (in the sample thickness) of the primary product concentrations ([P$^{\bullet}$], [PO$_2^{\bullet}$], [POOH], [PO$^{\bullet}{}^{\bullet}$OP]$_{cage}$, [PH], and [O$_2$]) and its evolution against time. Then, eqs. (7)–(9) were integrated against time to determine the spatial distribution of secondary product quantities ([P═O], [P—OH], and $\Delta m/m_0$) and its evolution against time. Finally, assuming that the sample thickness does not vary much during exposure, we determined the evolution of global secondary product quantities by summing the contribution of each elementary sublayer:

$$[y]_{glob}(t) = \frac{1}{2L}\int_{-L}^{L} [y](x,t)dx$$

where [y] = [P═O], [P—OH], or $\Delta m/m_0$ and $2L$ is the sample thickness.

Let us recall that secondary product quantities are very important from a practical point of view because they can be checked experimentally.

EXPERIMENTAL

Experiments were conducted on an unstabilized and unfilled, mainly isotactic (66%) PP powder provided by Priex Resins (Brussels, Belgium). Before aging tests, the as-received PP powder was characterized by IR spectrophotometry, differential scanning calorimetry (DSC), and steric exclusion chromatography (SEC). The main results are summarized in Table I.

Then, thick PP samples (4 mm thick) were processed by injection molding and microtome-cut into thin slices (40 μm thick) perpendicularly to the sample surfaces. Some PP slices were placed on KBr

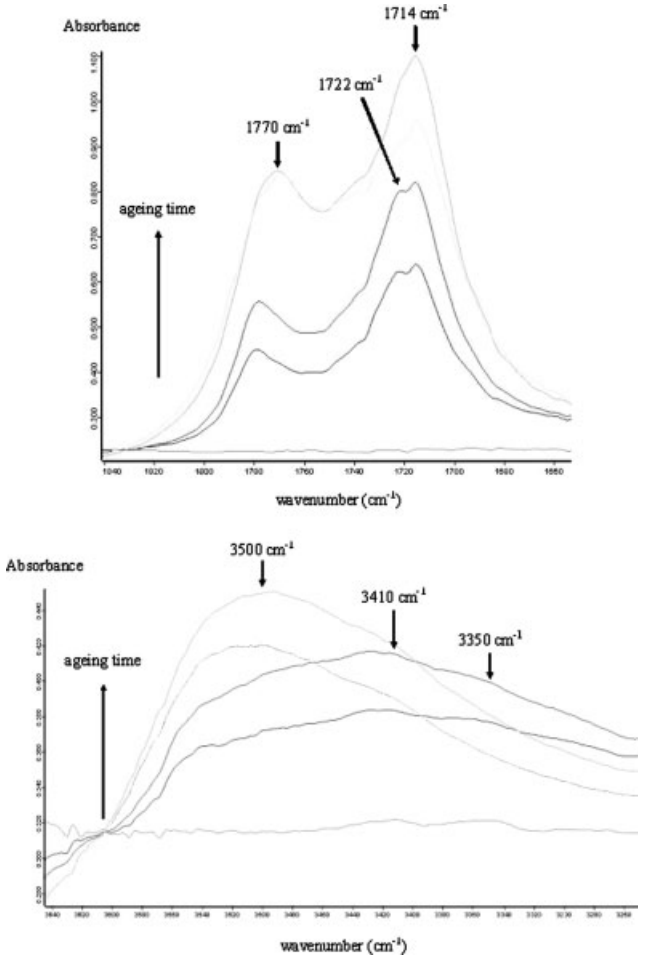

Figure 2 Changes in the carbonyl (above) and hydroxyl absorption bands (below) against the time of exposure (0, 10, 20, 30, and 60 min) for unstabilized PP films (40 μm thick) at 200°C in atmospheric air.

plates, exposed in ovens regulated at 190, 200, and 230 ± 1°C, and removed at defined aging times for physicochemical analysis. Some PP slices were analyzed with a Brucker IFS 28 IR (*Marne la vallée*, France) spectrophotometer, with a minimal resolution of 4 cm^{-1}, in a transmission mode to determine the ketone (at 1713–1722 cm^{-1})[25–28] and hydroxyl group (at 3378–3553 cm^{-1}) buildup.[29–31] As an example, the change versus the time of exposure of ketone and hydroxyl absorption bands at 200°C in atmospheric air is presented in Figure 2.

The global concentrations of ketone and hydroxyl groups were determined with the classical Beer–Lambert equation and the respective usual molar absorptivities:

$$[X] = \frac{DO}{2L\varepsilon}$$

where DO is the measured IR absorbance, $2L$ is the sample thickness (cm), and ε is the molar absorptivity of the chemical species under consideration: ε = 200 L mol^{-1} cm^{-1} for ketone[32] and ε = 70 L mol^{-1} cm^{-1} for hydroxyl groups.[33]

It must be noticed that, in contrast to the ketone absorption band, the hydroxyl one is badly defined: it is a wide composite band having several maxima, the most visible being located at 3410, 3415, and 3500 cm^{-1}.[20] Thus, the measured IR absorbance results from the sum of several contributions with respect to hydroperoxides, alcohols, carboxylic acids, and so forth. Moreover, the hydroxyl absorption band is relatively sensitive to humidity absorbed at the sample surface. Unfortunately, in our case, no precaution was taken to prevent any water uptake when the samples were removed from the ovens. All these uncertainties made it impossible to obtain correct experimental results. That is the reason why only kinetic curves of the ketone group concentration are simulated numerically hereafter.

Others PP slices, with an initial mass of approximately 2 mg, were placed on the plateau of a Netzsch TG 209 microbalance (*Selb/Bavière*, Germany). Their mass changes were determined at 190, 200, and 230 ± 1°C in atmospheric air with the following program: the samples were heated from the ambient temperature to the aging temperature at 50°C/min under a nitrogen flow of 10 mL/min, and after 1 min at the aging temperature for equilibration of the system, atmospheric air was admitted (10 mL/min). The sample masses were recorded continuously versus the time of exposure.

RESULTS AND DISCUSSION

Kinetic modeling under isothermal conditions

Experimental results obtained at 190, 200, and 230°C in atmospheric air are reported in Figures 3 and 4. All the kinetic curves display an induction period as expected when initiation by the direct addition of oxygen is negligible ($k_i = 0$) against hydroperoxide decomposition and also when the initial hydroperoxide

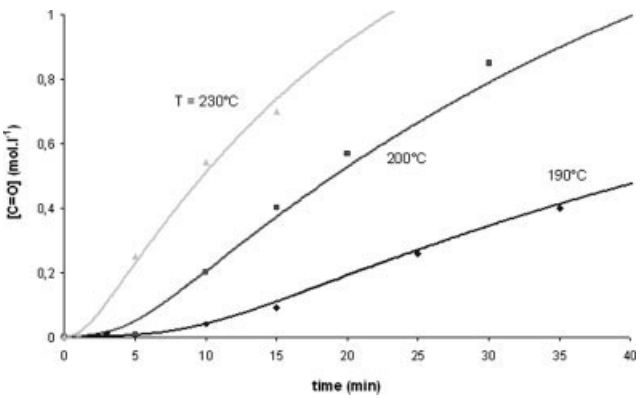

Figure 3 Kinetic curves of ketone group concentrations for unstabilized PP films (40 μm thick) at 190, 200, and 230°C in atmospheric air: a comparison of model predictions (continuous lines) and experimental data (points).

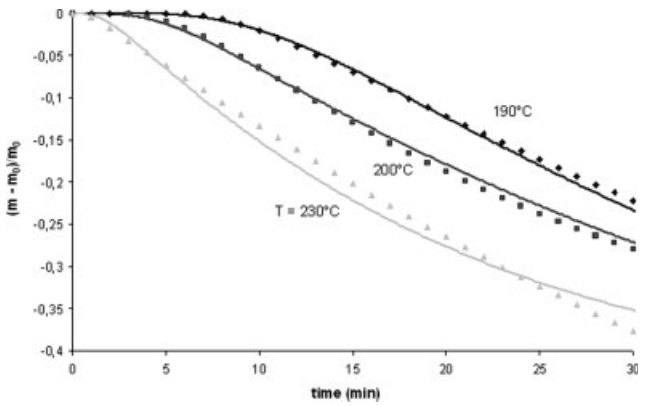

Figure 4 Kinetic curves of mass changes for unstabilized PP films (40 μm thick) at 190, 200, and 230°C in atmospheric air: a comparison of model predictions (continuous lines) and experimental data (points).

concentration is very small (typically $[POOH]_0 = 10^{-5}$–10^{-2} mol/L). For example, at 200°C, the duration of the induction period is about 4.5 min for mass changes and 5 min for ketones. It can thus be concluded that the sample preparation conditions, provided in the Experimental section, were correctly chosen to prevent any polymer preoxidation before thermal aging.

The kinetic model, composed of eqs. (1)–(9), was used to simulate mass changes and ketone buildup obtained at 190, 200, and 230°C in atmospheric air. The best simulations are reported in Figures 3 and 4. There is a good agreement between the model and the experimental results for mass changes and ketone group buildup at all temperatures.

As a result, it can be concluded that the model satisfactorily describes the thermal oxidation kinetics of molten unstabilized PP. Simulations at 200°C were obtained with the set of model parameters reported in Table II. Some model parameters were fixed before simulating the experimental results:

- The initial concentration of tertiary CH groups ($[PH]_0$) was determined from the PP theoretical structure:
  $[PH]_0 = 1/m$ where m is the molar mass of the monomer ($m = 42$ g/mol; i.e., $[PH]_0 = 23.8$ mol/kg or $[PH]_0 = 20.3$ mol/L if the density of molten PP is 854 g/L).
- Propagation rate constants k_2 and k_3 were determined from well-known structure–property relationships established for model compounds. The addition of oxygen to alkyl radicals (II) is very fast. The corresponding rate constant is very high: $k_2 = 10^8$–10^9 L mol^{-1} s^{-1}. Its activation energy is $E_2 \approx 0$.[13] Thus, in a first approximation, the value of $k_2 = 10^8$ L mol^{-1} s^{-1} was chosen for PP at 200°C. On the contrary, the rate of hydrogen abstraction by peroxyl radicals (III) depends on the dissociation energy (E_D) of the C—H bond involved. The Arrhenius parameters of the corresponding rate constant k_3 were determined from the Korcek relationships established for tertiary peroxyl radicals:[14]

$$E_3 = 0.55(E_D - 261.3) \quad \text{kJ/mol}$$

$$\text{Log}_{10}(k_3) = 15.4 - 4.79 \times 10^{-2} \times E_D \text{ L mol}^{-1}\text{s}^{-1} \text{ at } 30^\circ\text{C}$$

Using $E_D = 380$ kJ/mol for tertiary C—H bonds, we obtained the following:

$$k_3 = k_{30} \exp\left(-\frac{E_3}{RT}\right) = 3.0 \times 10^8 \exp\left(-\frac{65,500}{RT}\right) \quad \text{L mol}^{-1}\text{s}^{-1}$$

That is, $k_3 \approx 18$ L mol^{-1} s^{-1} for PP at 200°C.

- The equilibrium oxygen concentration ($[O_2]_S$) and oxygen diffusivity (D_{O2}) for molten PP were predicted from their respective values determined for semicrystalline PP above its glass-transition temperature and with knowledge of its crystallinity ratio (X_C):

$$[O_2]_{S,\text{melt}} = \frac{[O_2]_{S,\text{semi-cryst}}}{1 - X_C}$$

$$D_{O2,\text{melt}} = \frac{D_{O2,\text{semi-cryst}}}{1 - X_C}$$

where

$$[O_2]_{S,\text{semicryst}} = 6.7 \times 10^{-4} \text{ mol/L}$$ [34]

TABLE II
Parameter Values Used for the Modeling of PP Thermal Oxidation Kinetics at 200°C: A Comparison with Values Recently Published for PE[8,36]

	Polymer		
	PP	PE	Unit
k_{1u}	1×10^{-3}	2.8×10^{-3}	s^{-1}
k_{1b}	2×10^{-2}	7.2×10^{-3}	L mol^{-1} s^{-1}
$[POOH]_C$	5×10^{-2}	3.9×10^{-1}	mol/L
k_2	10^8	10^8	L mol^{-1} s^{-1}
k_3	18	1.3×10^2	L mol^{-1} s^{-1}
k_4	10^{10}	8×10^{11}	L mol^{-1} s^{-1}
k_5	10^9	2.3×10^{11}	L mol^{-1} s^{-1}
k_{60}	2×10^8	7.3×10^{10}	L mol^{-1} s^{-1}
k_{61}	5×10^6	2.0×10^6	s^{-1}
k_{63}	3×10^7	2.4×10^7	s^{-1}
γ_1	95.7	17	%
V	85	—	%
γ_4	16	50	%
γ_5	50	50	%

$$D_{O2,semi-cryst} = 2.3 \times 10^{-4} \exp\left(-\frac{47,700}{RT}\right) \quad m^2/s \ ^{35}$$

$$X_C = 50\%$$

From both relationships, $[O_2]_S \approx 1.3 \times 10^{-3}$ mol/L and $D_{O2} = 2.5 \times 10^{-9}$ m^2/s were obtained for PP at 200°C.

- In a first approach, it was assumed that acetone is the main volatile product formed during PP thermal oxidation in its liquid state. Therefore

$$M_V = 58\,g/mol, \quad n_{CO} = 1, \quad n_{OH} = 0, \quad \text{and} \quad n_{PH} = 0$$

- Finally, $[POOH]_0$ was measured by iodometric titration of the reaction between iodide ions (I^-) and O—O bonds from hydroperoxides in an acidified environment according to the following equations:

$$2I^- + 2H^+ + POOH \rightarrow POH + H_2O + I_2$$

$$I_2 + I^- \rightarrow I_3^-$$

$$POOH + 3I^- + 2H^+ \rightarrow POH + I_3^- + H_2O$$

I_3^- ions, produced in the same quantity as consumed POOH, were detected by the consideration of their UV absorption at 355 nm. Then, $[POOH]_0 = 1.07 \times 10^{-2}$ mol/L.

All other parameters were determined with the model used as an inverse method based on a trial and error procedure. Their values at 200°C are compared to those recently published for PE[8–36] in Table II. These values seem to be physically reasonable. They call for the following comments:

1. The relative importance of unimolecular and bimolecular hydroperoxide decomposition can be appreciated if we consider the critical hydroperoxide concentration ($[POOH]_C$) corresponding to the equality of the rates of both processes:

$$[POOH]_C = k_{1u}/k_{1b} = 5 \times 10^{-2}\,mol/L$$

The inverse approach led to a value of $[POOH]_C$ 5 times higher than the initial hydroperoxide concentration ($[POOH]_0 \approx 10^{-2}$ mol/L) but also 3 times lower than the maximal hydroperoxide concentration ($[POOH]_S \approx 1.6 \times 10^{-1}$ mol/L) reached in the pseudo-steady-state regime. In other words, bimolecular decomposition always remains predominant over unimolecular decomposition for PP at 200°C. Moreover, PP hydroperoxides are 3 times more unstable than PE ones at 200°C: $k_{1b,PP} \approx 3 \times k_{1b,PE}$ at 200°C. This result agrees well with those previously reported for model compounds at lower temperatures. As an example, Reich and Stivala[37] obtained the following equality between the rate constants of bimolecular decomposition of tertiary (terPOOH) and secondary hydroperoxides (secPOOH):

$$k_{1b,terPOOH} \approx 5 - 6 \times k_{1b,secPOOH} \text{ at } 45 - 55°C$$

2. Termination rate constants well respect the theoretical hierarchy: $k_4 > k_5 > k_{60}$. Moreover, these rate constants are 2 orders of magnitude lower in PP than in PE at 200°C:

$$k_{4,PE} \approx 80 \times k_{4,PP}, \quad k_{5,PE} \approx 230 \times k_{5,PP}, \quad \text{and} \quad k_{60,PE} \approx 360 \times k_{60,PP}$$

Once again, these results agree well with those previously reported for model compounds at lower temperatures. As an example, Howard and Ingold[38] obtained the following classification of rates of bimolecular peroxyl radical terminations:

$$\text{Tertiary peroxyl} < \text{Secondary peroxyl} < \text{Primary peroxyl radicals}$$

As another example, a compilation of literature data leads to the following equality between the rate constants of bimolecular terminations of tertiary ($terPO_2^\bullet$) and secondary peroxyl radicals ($secPO_2^\bullet$):[39,40]

$$k_{t,sec\,PO2\bullet} \approx 430 - 1150 \times k_{t,terPO2\bullet} \text{ at } 30°C$$

3. On the contrary, no significant differences have been obtained between the rate constants k_{61} and k_{63} for PP and PE.[36] It seems that the corresponding elementary reactions are practically independent of the radical structure involved.
4. The fact that γ_1 is close to unity means that the rearrangement of alkoxyl radicals by β scission is very efficient in the liquid state. It can be thus concluded that hydroxyl groups come essentially from hydroperoxide species for PP at 200°C.

Simulations were also made at 190 and 230°C. The values of model parameters obtained at both temperatures are reported in Table III.

Acetone detection

In a first approach, it was assumed that acetone is the main volatile product formed during PP thermal

TABLE III
Parameter Values Used for the Modeling of PP Thermal Oxidation Kinetics at 190, 200, and 230°C

	Temperature			
	190°C	200°C	230°C	Unit
k_{1u}	5×10^{-4}	1×10^{-3}	9×10^{-3}	s^{-1}
k_{1b}	6×10^{-3}	2×10^{-2}	4×10^{-2}	L mol^{-1} s^{-1}
$[POOH]_C$	8.3×10^{-2}	5×10^{-2}	2.3×10^{-1}	mol/L
k_2	10^8	10^8	10^8	L mol^{-1} s^{-1}
k_3	12	18	47	L mol^{-1} s^{-1}
k_4	10^{10}	10^{10}	10^{10}	L mol^{-1} s^{-1}
k_5	10^9	10^9	10^9	L mol^{-1} s^{-1}
k_{60}	8×10^7	2×10^8	5×10^8	L mol^{-1} s^{-1}
k_{61}	4.2×10^6	5×10^6	5×10^6	s^{-1}
k_{63}	5×10^7	3×10^7	8×10^7	s^{-1}
γ_1	90	95.7	99.9	%
V	84.7	85	88	%
γ_4	16	16	16	%
γ_5	50	50	50	%

oxidation. To check this assumption, a particularly suitable analytical tool for complex mixtures of volatile compounds diluted in air has recently appeared: proton transfer reaction (PTR) associated with Fourier transform ion cyclotron resonance mass spectrometry (FTICRMS).[41] The principle of this recently developed method can be summarized as follows: a gas phase reaction of the volatile compounds contained in a sample with H_3O^+ ions generates protonated volatile compounds by proton exchange. These ions are mass-analyzed in an FTICRMS apparatus, which measures the molar mass to charge ratio (m/z) of ions and generates a mass spectrum figuring the relative amount of each ion as a function of m/z. Each component A of molecular mass M of the volatile compound mixture leads to the ion AH^+, which corresponds to a peak at $m/z = M + 1$ on the mass spectrum. Because of the remarkable mass resolution and accuracy of FTICRMS, the molecular formulas of the analytes are reliably determined.

An unstabilized PP film, with a thickness of 40 μm and a mass of 2.8 mg, was introduced into a tubular furnace first heated at 230°C under a dry atmospheric air flow of 40 mL/min. Every 5 s, a small volume of gases was removed from the furnace and analyzed by FTICRMS.

Four main volatile products were distinguished: protonated acetone ($C_3H_6O^+$; $m/z = 59$), acetaldehyde ($C_2H_4O^+$; $m/z = 45$), formaldehyde (CH_2O^+; $m/z = 31$), and methyl acrolein ($m/z = 71$) appear as separate signals during the exposure of PP. Their concentration is expressed in parts per million (number of moles among 10^9 mol of gas molecules) and plotted versus the time of exposure in Figure 5.

As previously observed by other authors in the solid state,[21,22] here, in the liquid state, acetone is also by far the main compound. Indeed, it represents more than 55 mol % of the total amount of generated gases.

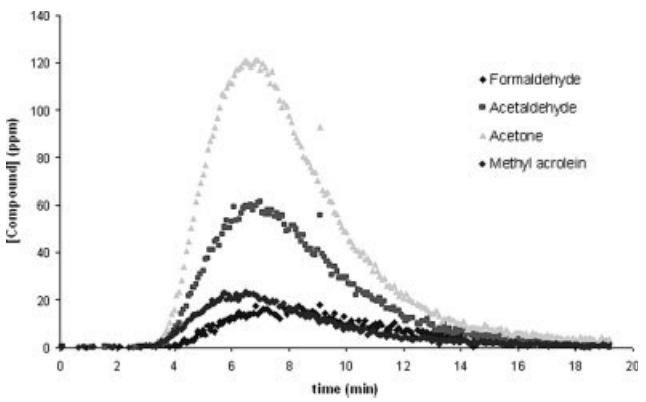

Figure 5 Main volatile organic compounds detected by PTR–FTICRMS. Protonated acetone ($C_3H_7O^+$; $m/z = 59$), acetaldehyde ($C_2H_5O^+$; $m/z = 45$), formaldehyde (CH_3O^+; $m/z = 31$), and methyl acrolein ($C_4H_7O^+$; $m/z = 71$) appear as separate signals during the exposure of unstabilized PP films (40 μm thick) at 230°C in atmospheric air.

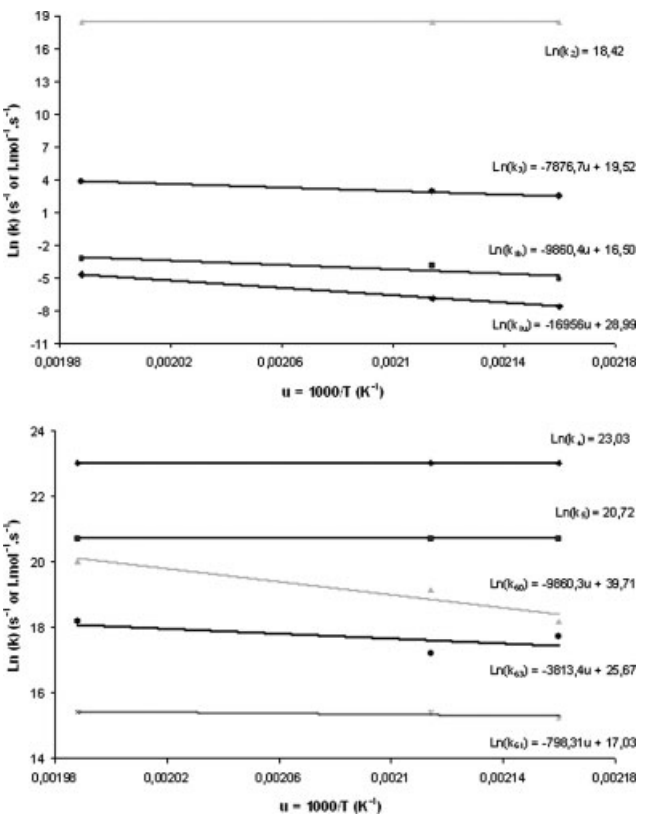

Figure 6 Determination of the Arrhenius parameters of the elementary rate constants for PP thermal oxidation kinetics between 190 and 230°C: initiation and propagation rate constants (top) and radical bimolecular combination rate constants (bottom).

TABLE IV
Arrhenius Parameter Values of Elementary Rate Constants for PP Thermal Oxidation Kinetics Between 190 and 230°C

Parameter	E_a (kJ/mol)	k_0 (s^{-1} or L mol^{-1} s^{-1})
k_{1u}	141	3.9×10^{12}
k_{1b}	82	1.5×10^{7}
k_2	0	10^{8}
k_3	65.5	3.0×10^{8}
k_4	0	10^{10}
k_5	0	10^{9}
k_{60}	82	1.8×10^{17}
k_{61}	6.6	2.5×10^{7}
k_{63}	31.7	1.4×10^{11}

E_a = activation energy; k_0 = pre-exponential factor.

Activation energies and pre-exponential factors

The Arrhenius parameters of the different elementary rate constants were determined graphically, as shown in Figure 6. Their values are reported in Table IV.

The orders of magnitude of the activation energies and pre-exponential factors correspond well to those previously reported in the literature.[8,9,36,42] As an example, for unimolecular ($1u$) and bimolecular ($1b$) hydroperoxide thermal decompositions, the obtained values confirm well the following inequalities:

- $E_{1u} > E_{1b}$
  where $E_{1u} \sim$ 120–140 kJ/mol and $E_{1b} \sim$ 80–120 kJ/mol.
- $k_{1u0} > k_{1b0}$
  where $k_{1u0} \approx 10^{11}$–10^{13} s^{-1} and $k_{1b0} \sim 10^{9}$–10^{11} L mol^{-1} s^{-1}.

Moreover, for bimolecular combinations of radicals, the obtained values well confirm the following hierarchy:

- $E_{63} > E_{61} > E_5 \geq E_4$
  where $E_{63} \sim$ 20–50 kJ/mol, $E_{61} \sim$ 0–20 kJ/mol, and $E_5 \sim E_4 \sim 0$ kJ/mol.
- $k_{40} > k_{50}$ and $k_{630} \gg k_{610}$
  where $k_{40} \sim k_{50} \sim 10^{8}$–$10^{11}$ L mol^{-1} s^{-1}, $k_{630} \approx 10^{9}$–10^{13} s^{-1}, and $k_{610} \sim 10^{4}$–10^{8} s^{-1}.

CONCLUSIONS

The first objective of our study was to build a nonempirical kinetic model for the thermal oxidation of molten unstabilized PP, which typically occurs at 170–250°C, a current temperature range for PP processing. A kinetic model has been derived from a realistic mechanistic scheme in which the volatile product formation is detailed. This model simulates accurately the kinetic curves of mass changes and ketone group buildup at 190, 200, and 230°C in atmospheric air. A set of physically reasonable model parameters has been determined, with the model used as an inverse method, and successfully compared to that recently published for PE. As a result, the validity of the kinetic model has been considered successfully checked between 190 and 230°C.

An extension of this model in a larger temperature range is in progress at the laboratory. Possible extension limits could be as follows:

- At lower temperatures, the presence of a physical state transition, such as the melting transition (≈165°C).
- At higher temperatures (typically >250°C), the existence of new degradation mechanisms, such as polymer thermolysis.

References

1. Boss, C. R.; Chien, J. C. W. J Polym Sci Part A-1: Polym Chem 1966, 4, 1543.
2. Billingham, N. C.; Calvert, P. D. In Developments in Polymer Stabilization; Scott, G., Ed.; Applied Science: London, 1980; p 139.
3. Gillen, K. T.; Wise, J.; Clough, R. L. Polym Degrad Stab 1995, 47, 149.
4. Verdu, S.; Verdu, J. Macromolecules 1997, 30, 2262.
5. Audouin, L.; Achimsky, L.; Verdu, J. Handbook of Polymer Degradation, 2nd ed.; Marcel Dekker: New York, 2000; p 727.
6. Rincon-Rubio, L.; Fayolle, B.; Audouin, L.; Verdu, J. Polym Degrad Stab 2001, 74, 177.
7. Richaud, E.; Farcas, F.; Bartoloméo, P.; Fayolle, B.; Audouin, L.; Verdu, J. Polym Degrad Stab 2006, 91, 398.
8. Colin, X.; Audouin, L.; Verdu, J. Polym Degrad Stab 2004, 86, 309.
9. (a) Colin, X.; Audouin, L.; Verdu, J. Polym Degrad Stab 2007, 92, 886; (b) Colin, X.; Audouin, L.; Verdu, J. Polym Degrad Stab 2007, 92, 898; (c) Colin, X.; Audouin, L.; Verdu, J. Polym Degrad Stab 2007, 92, 906.
10. Gonzales-Gonzales, V. A.; Neira-Velasquez, G.; Angulo-Sanchez, J. L. Polym Degrad Stab 1998, 60, 33.
11. Xiang, Q.; Xanthos, M.; Miltra, S.; Patel, S. H.; Guo, J. Polym Degrad Stab 2002, 77, 93.
12. (a) Bolland, J. L.; Gee, G. Trans Faraday Soc 1946, 42, 236; (b) Bolland, J. L.; Gee, G. Trans Faraday Soc 1946, 42, 244.
13. Kamiya, Y.; Niki, E. In Aspect of Degradation and Stabilisation of Polymers; Jellinek, H. H. G., Ed.; Elsevier: New York, 1978; Chapter 3, p 86.
14. Korcek, S.; Chenier, J. H. B.; Howard, J. A.; Ingold, K. U. Can J Chem 1972, 50, 2285.
15. Colin, X.; Fayolle, B.; Audouin, L.; Verdu, J. Polym Degrad Stab 2003, 80, 67.
16. Uri, N. In Autoxidation and Antioxidants; Lundberg, W. O., Ed.; Wiley: New York, 1961; Chapter 2, p 62.
17. Reich, L.; Stivala, S. S. In Autoxidation of Hydrocarbons and Polyolefins, Kinetics and Mechanisms; Marcel Dekker: New York, 1969; Chapter 2, p 110.
18. Pryor, W. A. Free Radicals; McGraw-Hill Series in Advanced Chemistry; McGraw-Hill: New York, 1969; Chapter 17, p 280.
19. Khelidj, N.; Colin, X.; Audouin, L.; Verdu, J.; Monchy-Leroy, C.; Prunier, V. Polym Degrad Stab 2006, 91, 1593.

20. Achimsky, L. Ph.D. Thesis, ENSAM Ecole Nationale Supérieure d'Arts et Métiers, Paris, France, 1996; p 122.
21. Wunderlich, B. Macromolecular Physics; Academic: New York, 1980; Vol. 3, p 61.
22. Barabas, K.; Iring, M.; Laszlo-Hedvig, S.; Kelen, T.; Tudos, F. Eur Polym J 1978, 14, 405.
23. Coquillat, M.; Verdu, J.; Colin, X.; Audouin, L.; Neviere, R. Polym Degrad Stab 2007, 92, 1334.
24. Severini, F.; Gallo, R.; Ipsale, S. Polym Degrad Stab 1988, 22, 185.
25. Teissèdre, G.; Pilichowski, J. F.; Lacoste, J. Polym Degrad Stab 1995, 45, 145.
26. George, G. A.; Celina, M.; Vassallo, A. M.; Cole-Clarke, P. A. Polym Degrad Stab 1995, 48, 199.
27. Adams, J. H. J Polym Sci Part A-1: Polym Chem 1970, 8, 1077.
28. Lacoste, J.; Vaillant, D.; Carlsson, D. J. J Polym Sci Part A: Polym Chem 1993, 31, 715.
29. Chien, J. C. W.; Vandeberg, E. J.; Jabloner, H. J Polym Sci Part A-1: Polym Chem 1968, 6, 393.
30. Chien, J. C. W. Polymer Stabilization; Wiley: New York, 1972; Chapter 5, p 95.
31. Mair, D.; Hall, R. T. In Organic Peroxides; Swern, D., Ed.; Wiley: New York, 1971; Vol. 2, Chapter VI, p 535.
32. Heacok, J. J Appl Polym Sci 1963, 7, 2319.
33. Tabankia, M.; Phillipart, J.; Gardette, J. Polym Degrad Stab 1985, 12, 349.
34. Van Krevelen, D. W.; Hoftyzer, P. J. Properties of Polymers: Their Estimation and Correlation with Chemical Structure, 2nd ed.; Elsevier: Amsterdam, 1976; p 407.
35. Stannet, V. In Diffusion in Polymers; Crank, J.; Park, G. S., Eds.; Academic: New York, 1968; p 41.
36. Khelidj, N.; Colin, X.; Audouin, L.; Verdu, J.; Monchy-Leroy, C.; Prunier, V. Polym Degrad Stab 2006, 91, 1598.
37. Reich, L.; Stivala, S. S. Autoxidation of Hydrocarbons and Polyolefins, Kinetics and Mechanisms; Marcel Dekker: New York, 1969; Chapter 2, p 56.
38. Howard, J. A.; Ingold, K. U. Can J Chem 1967, 45, 793.
39. Kamiya, Y.; Niki, E. In Aspect of Degradation and Stabilisation of Polymers; Jellinek, H. H. G., Ed.; Elsevier: New York, 1978; Chapter 3, p 87.
40. (a) Howard, J. A.; Ingold, K. U. Can J Chem 1968, 46, 2655; (b) Howard, J. A.; Ingold, K. U. Can J Chem 1968, 46, 2661.
41. Sarrabi, S.; Colin, X.; Tcharkhtchi, A.; Heninger, M.; Mestdagh, H.; Leprovost, J. Int J Mass Spectrosc, submitted.
42. Coquillat, M. Ph.D. Thesis, ENSAM, 2007; p 123.